

# Influence of Coulomb interaction on the Aharonov-Bohm effect in an electronic Fabry-Pérot interferometer

Stéphane Ngo Dinh<sup>1</sup> and Dmitry A. Bagrets<sup>2,3</sup>

<sup>1</sup>*Institut für Theorie der Kondensierten Materie and DFG Center for Functional Nanostructures, Karlsruhe Institute of Technology, 76128 Karlsruhe, Germany*

<sup>2</sup>*Institut für Nanotechnologie, Karlsruhe Institute of Technology, 76021 Karlsruhe, Germany*

<sup>3</sup>*Institut für Theoretische Physik, Universität zu Köln, Zùlpicher Str. 77, 50937 Köln, Germany*

(Dated: November 20, 2018)

We study the role of Coulomb interaction in an electronic Fabry-Pérot interferometer (FPI) realized with chiral edge states in the integer quantum Hall regime in the limit of weak backscattering. Assuming that a compressible Coulomb island in a bulk region of the FPI is formed, we develop a capacitance model which explains the plethora of experimental data on the flux and gate periodicity of conductance oscillations. It is also shown that a suppression of finite-bias visibility stems from a combination of weak Coulomb blockade and a nonequilibrium dephasing by the quantum shot noise.

PACS numbers: 71.10.Pm, 73.23.-b, 73.43.-f, 85.35.Ds

Electron interferometry provides a powerful tool for studying the quantum interference and dephasing in mesoscopic semiconductor devices. Notably, the 2DEG placed in the quantum Hall effect (QHE) regime has been proved to be highly tailored to realize electronic analogues of optical interferometers, such as Fabry-Pérot (FPI) [1–4] and Mach-Zehnder (MZI) [5] interferometers, with chiral edge states playing the role of light beams and quantum point contacts (QPCs) serving as beam splitters. These experimental efforts are motivated by the recent interest in topological quantum computations, which propose to exploit the non-Abelian anyons in the fractional QHE regime [6].

The Coulomb interaction is of paramount importance in fractional QHE systems where it gives rise to quasiparticles with fractional charge obeying anyonic statistics. It came as a surprise that  $e$ - $e$  interaction plays a prominent role in the integer QHE interferometers as well, even when their conductance is  $\sim e^2/h$  so that Coulomb blockade physics seems to be inessential. Experiments realizing MZIs and FPIs in this limit can not be explained by means of the non-interacting Landauer-Büttiker scattering approach applied to chiral edge states. The search for a resolution of this puzzle in the case of MZI has triggered a lot of attention. On the contrary, the extent of theoretical works on FPIs operat-

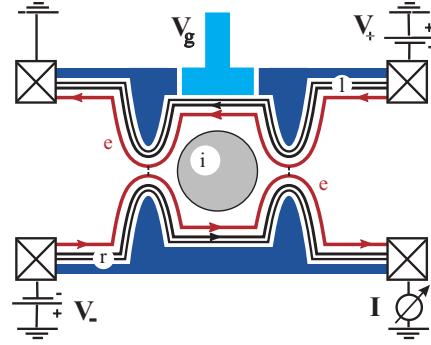


FIG. 1: Fabry-Pérot interferometer with a center compressible island “ $i$ ”. The innermost edge channels “ $e$ ” are subject to backscattering at the QPCs; the remaining  $f_T = \nu - 1$  right( $r$ )- and left( $l$ )- moving channels are fully transmitted.

ing in the integer QHE regime is rather small [7–9], and a theory for non-equilibrium edge-state dephasing in these devices has not been elaborated in detail.

In this paper we propose a minimal capacitance model of  $e$ - $e$  interaction in the FPI and apply it to study its transport properties in- and out-of-equilibrium in the limit of weak backscattering. Our approach is inspired by the previous theoretical work [8]. Its essential idea is that in the center of the FPI between two constrictions a compressible Coulomb island can be formed (Fig. 1) which strongly affects Aharonov-Bohm oscillations.

We show, that depending on the strength of inter-channel  $e$ - $e$  interaction  $\alpha = e^2/(\hbar v_D)$ , with  $v_D$  being the drift velocity, and on the ratio of gate-to-island ( $C_{gi}$ ) to edge-to-island capacitance ( $C_{ei}$ ) the FPI can fall into “Aharonov-Bohm” (AB) or “Coulomb-dominated” (CD) regimes observed in the experiments [2, 4] (Table I), including the “exotic” behavior discovered in [4], which we classify as the type II CD regime. There is a partial overlap of our results at equilibrium with recent work [9]. We also analyze the suppression of AB oscillations out-

TABLE I: “Phase diagram” of the FPI (for definitions of inter-channel interaction  $\alpha$  and capacitances  $C_{gi}$ ,  $C_{ei}$ , see text). The AB regime in the limit of  $\alpha \gg 1$  (“?”) was not observed.

	$C_{gi}/C_{ei} \ll 1$	$C_{gi}/C_{ei} \gg 1$
$\alpha \gg \ln(w/a)$ , $\nu^* \simeq 1$	CD, type I	?
$\alpha \ll \ln(w/a)$ , $\nu^* \simeq \nu$	CD, type II	AB

of-equilibrium with the increase of a source-drain voltage and find both power-law and exponential decays, which may explain experiments of Refs. [1, 3].

*Model* — We consider an electronic FPI of size  $L$  formed by a Hall bar with  $\nu$  edge channels and two constrictions (QPCs) that allow for electron backscattering between the innermost right-/left-moving edge channels with amplitudes  $r_{1(2)}$  as shown in Fig. 1.

According to Chklovskii *et al.* [10], the 2DEG in the QHE regime is divided into compressible and incompressible strips (if  $w$  and  $a$  are their typical widths, then  $w \gg a \gg \lambda_B$ , with  $\lambda_B$  being the magnetic length). Compressible regions play the role of edge channels separated by narrow insulating stripes of the incompressible 2DEG. We assume that the filling fraction in the center of the FPI exceeds  $\nu$  giving rise to a compressible droplet (Coulomb island). The reason for that can be smooth (on a scale  $\lambda_B$ ) disorder potential fluctuations [11].

We take  $e$ - $e$  interaction in the FPI into account using the constant interaction model with mutual capacitances between four compressible regions — the interfering channel ( $e$ ); right- and left-moving fully transmitted channels ( $r$ ,  $l$ ); the compressible island ( $i$ ) — and the gate ( $g$ ). One estimates them as  $C_{r(l)e} \sim \epsilon L \ln(w/a)$ ,  $C_{r(l)i} \sim \epsilon r \ln(r/a)$ ,  $C_{eg} \sim \epsilon w L/d$  and  $C_{ig} \sim \epsilon r^2/d$  with  $d$  being a depth of 2DEG below a top gate, and we take the droplet to be a disk of size  $r \simeq L$ . We assume a large capacitance between counter-propagating innermost channels — thus they share the same electrostatic potential  $\varphi_e$  — and also consider  $f_T$  right- and left-moving channels as joint conductors with potentials  $\varphi_r$  ( $\varphi_l$ ). Defining a capacitance matrix  $\tilde{C}$  with elements  $\tilde{C}_{\alpha\alpha} = \sum_{\gamma} C_{\alpha\gamma} + C_{\alpha g}$ , and  $\tilde{C}_{\alpha\beta} = -C_{\alpha\beta}$  ( $\alpha \neq \beta$ ), where Greek indices span the set  $\{e, r, l, i\}$  and  $q_\alpha = -C_{\alpha g} V_g$  is an offset charge on the  $\alpha$ 's conductor, the electrostatic energy reads

$$E = (1/2) \sum_{\alpha\beta} (Q_\alpha - q_\alpha) \left( \tilde{C}^{-1} \right)_{\alpha\beta} (Q_\beta - q_\beta). \quad (1)$$

Here the total charge on the island,  $Q_i = e(N_i + \nu\phi/\phi_0)$ , is contributed by the highest partially filled Landau level (LL) and  $\nu$  fully occupied underlying LLs [8]. With  $N_i$  being integer, the former part of this charge is quantized;  $\phi$  stands for a magnetic flux through the FPI and  $\phi_0 = hc/|e|$  is the flux quantum (we take a convention  $e < 0$ ).

*Results* - In the weak backscattering limit  $r_j \ll 1$ , the dependence of the AB conductance on external parameters — the gate voltage  $V_g$ , the variation of magnetic field  $\delta B$  and the bias  $V = V_+ - V_-$  — factorizes into

$$g_{AB}(V, V_g, \delta B) = g(V) \cos[\varphi_{AB}(V_g, \delta B)], \quad (2)$$

where the AB phase  $\varphi_{AB}$  will be discussed shortly and

$$g(V) = 2e^{-\tau/\tau_\varphi(V)} R_{12*}(V) |\cos(|eV\tau| - \pi/4\nu^*)|. \quad (3)$$

Here  $\tau = L/v_D$  is the flight time of electrons through the FPI,  $\nu^*$  is the effective number of channels participating

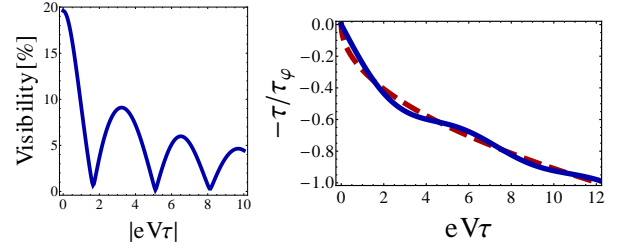


FIG. 2: (Left) visibility of AB oscillations,  $g(V)/\nu$ ; (Right) dephasing rate as a function of source-drain voltage, the dashed line is the power-law asymptotic given by Eq. (4). Parameters are  $\nu^* = 2$ ,  $\omega_C \tau = 25$ ,  $R_{1*}(\epsilon_{\text{Th}}) = R_{2*}(\epsilon_{\text{Th}}) = 0.2$ .

in screening  $-\nu^* \simeq 1$  in the case of strong inter-channel coupling  $\alpha \gg \ln(w/a)$  while  $\nu^* \simeq \nu$  in the weak coupling limit  $-$ , and the nonequilibrium dephasing rate

$$\tau_\varphi^{-1} = (2/\pi) |eV| (R_{1*}(V) + R_{2*}(V)) \sin^2(\pi/2\nu^*). \quad (4)$$

There are two characteristic energy scales in our problem,  $\epsilon_{\text{Th}} = \pi/\tau$  being the Thouless energy and  $\omega_C$  being the charge relaxation rate, where  $\epsilon_{\text{Th}} \ll \omega_C$ . In the range  $\epsilon_{\text{Th}} \ll |eV| \ll \omega_C$  the renormalized reflection coefficients behave as  $R_{j*} \propto V^{-1/\nu^*}$  and  $R_{12*} \propto V^{-1/2\nu^*}$  where one sets  $R_{j*} \simeq |r_j|^2$  and  $R_{12*} \simeq |r_1 r_2|$  at high energy scale  $\omega_C$ . This renormalization comes from *virtual* electron-hole excitations (being a precursor of weak Coulomb blockade [12]) and stops at  $eV \simeq \epsilon_{\text{Th}}$ , whereas  $\tau_\varphi^{-1}$  is caused by *real* e-h pairs excited by backscattered electrons and is proportional to the shot noise of the QPCs. As the function of bias, the amplitude (3) of AB oscillations shows the “lobe” structure (Fig. 2) on a scale of the Thouless energy  $\epsilon_{\text{Th}}$  in agreement with Refs. [1, 3].

In experiment one usually characterizes the FPI in terms of a pattern of its equilibrium conductance in  $(B, V_g)$ -plane, which is governed by AB phase. Defining island and edge capacitances as  $\bar{C}_i = \bar{C}_{ei} + C_{ig}$  and  $\bar{C}_e = \bar{C}_{eg} + \bar{C}_{ei} C_{ig} / \bar{C}_i$  respectively, where  $\bar{C}_{ei} = C_{ei} + C_{ri} + C_{li}$  (and similarly for  $\bar{C}_{eg}$ ), we have found that

$$\varphi_{AB} = 2\pi\phi/\phi_0 - \frac{2\pi}{\nu^*} \frac{\bar{C}_{ei}}{\bar{C}_i} (N_i + \nu\phi/\phi_0) + |e| (2V_g - V_+ - V_-) / \omega_C. \quad (5)$$

Here  $\phi = A\delta B$  is the variation of the flux through some reference loop area,  $\omega_C = \nu^* e^2 / (\pi \bar{C}_e)$  is the charge relaxation rate, and  $N_i$  minimizes the charging energy

$$E_i = \frac{e^2}{2\bar{C}_i} \left( N_i + \nu\phi/\phi_0 - C_{ig} V_g / |e| \right)^2. \quad (6)$$

*Discussion* - Importantly, Eq. (5) can be interpreted in terms of variation of the relevant FPI's area when the magnetic field and voltage are varied [4]. Representing the magnetic flux as  $\Phi = B \cdot A(V_g, B)$ , this leads to

$$\left( \frac{\partial A}{\partial B} \right)_{V_g} = -\frac{\nu}{\nu^*} \left( \frac{\bar{C}_{ei}}{\bar{C}_i} \right) \frac{A}{B}, \quad \left( \frac{\partial A}{\partial V_g} \right)_B = \frac{|e|}{\omega_C} \frac{\phi_0}{\pi B}, \quad (7)$$

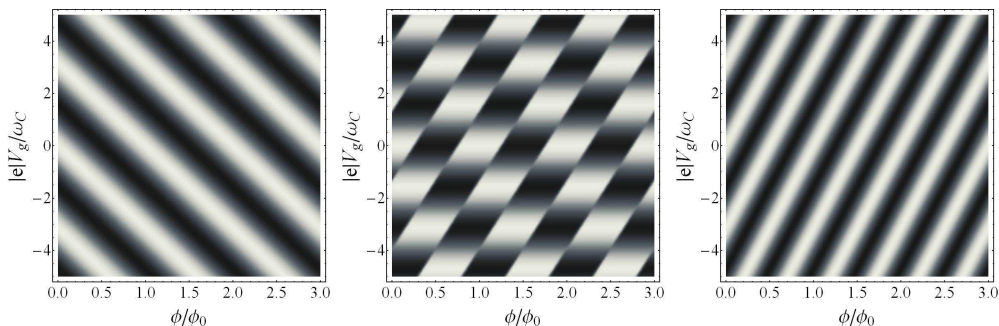


FIG. 3: AB conductance: AB regime (left),  $\nu = 2$ ; type-II CD (middle),  $\nu = 2$ ,  $C_{ig}/\bar{C}_e = 0.6$ ; type-I CD (right),  $\nu = 3$ .

i.e. a qualitative dependence of  $A(B, V_g)$  on the parameters  $\nu^*$  and  $\bar{C}_{ei}/\bar{C}_i$  and hence on the different regimes of Table I. The corresponding patterns of AB conductance are shown in Fig. 3.

In the AB regime the magnetic field period is  $\Delta B = \phi_0/A$  and the area of the FPI does not change with  $B$  yielding the lines of constant phase with a negative slope (Fig. 3, left). This regime is observed in large devices (cell area  $\sim 20\mu\text{m}^2$ ) with a top gate [1, 2, 4], where the condition  $\bar{C}_{ei} \ll C_{gi}$  is satisfied. Assuming that  $\bar{C}_e \simeq \bar{C}_{ei} + \bar{C}_{eg}$  is  $\nu$ -independent, one obtains a gate period  $\Delta V_g = \pi\omega_C/e \propto 1/B$ , consistent with Ref. [2].

To distinguish between type-I and II CD regimes we compare an inter-channel interaction energy  $e^2/C_{re}$  with the Thouless energy  $\sim v_D/L$ . Using the estimate for  $C_{re}$  one gets a crossover value for the coupling constant  $\alpha^* \sim \ln(w/a)$ . In the CD regime one has  $\bar{C}_{ei}/\bar{C}_i \simeq 1$  and the area of the interfering loop shrinks with the increase of magnetic field. In the type-II regime such shrinkage exactly compensates a change in “naïve” AB phase  $\phi = A\delta B$ , which causes the true AB phase to stay piecewise constant while keeping  $V_g$  fixed. When the FPI is brought close to a charge degeneracy point of the island by varying  $V_g$  or  $B$ , electron tunneling becomes possible between the droplet and interfering channels resulting in abrupt change of  $A$ . This creates a phase lapse  $\Delta\phi_{AB} = \pm 2\pi/\nu$  giving rise to the “rhomb-like” pattern shown in Fig. 3 (middle) at  $\nu \geq 2$ . Such “exotic” behaviour of AB oscillations has been reported in Ref. [4].

In the type-I CD regime a change in AB phase caused by area shrinkage when rising  $B$  overcompensates the “naïve” AB phase. At the same time, whenever an electron tunnels into the island, the interfering edges contract so as to expell exactly one flux quantum from the AB loop (the phase lapse  $\Delta\phi_{AB} = \pm 2\pi$ ), which is invisible in the interference conductance. This leads to the diagonal stripe pattern (Fig. 3, right) with periodicities  $\Delta B = \phi_0/(f_TA)$  and  $\Delta V_g = e/(C_{ei} + C_{gi})$  and lines of constant phase having positive slope (at  $\nu = 1$  lines are vertical) (cf. Ref.[8]) The above scenario has been realized in Refs. [2, 4] for small FPIs (area  $2 \div 5\mu\text{m}^2$ ), where a presence/absence of a top gate did not affect their be-

havior, suggesting the CD limit  $C_{ei} \gg C_{gi}$ .

*Calculations* - We now turn to sketch our calculations the details of which will be published separately. The FPI is modeled by 1D chiral fermions, interacting according to Eq. (1). We use the functional bosonization framework [13] and decouple interaction by means of electrostatic potentials  $\varphi_\alpha(t)$  with Lagrangian

$$\mathcal{L}_0 = \sum_{\langle\alpha\beta\rangle} \frac{C_{\alpha\beta}}{2} (\varphi_\alpha - \varphi_\beta)^2 + \sum_{\alpha \neq g} \frac{C_{\alpha g}}{2} (\varphi_\alpha - V_g)^2 - \varphi_i Q_i \quad (8)$$

Along the lines of Ref. [14] one can now integrate out the fermions to obtain the Keldysh action describing electron scattering in the FPI:

$$i\mathcal{A}_{\text{FPI}}[\varphi] = \ln \text{Det} [\mathbf{1} + (S[\varphi^b]^\dagger S[\varphi^f] - \mathbf{1}) f]. \quad (9)$$

This result bears close relation to the problem of electron full counting statistics [15]. The determinant is to be taken with respect to time and channel indices  $\mu$ ;  $f_{\lambda\mu} = \delta_{\lambda\mu} f_\mu^< = ie^{-ieV_\mu t}/2\pi(t+i0)$  are zero temperature occupation numbers in the incoming channels and  $S_{\lambda\mu}[\varphi^{f/b}](t, t')$  is the time-dependent single-particle scattering matrix of the FPI in the potential  $\varphi^{f/b}$  on two branches of the Keldysh contour  $\mathcal{C}$ . It can be constructed using the scattering matrices of the QPCs and the transfer matrix  $\mathcal{M}_\pm(t, t_0) = e^{i\theta_\pm(t) + i\phi_\pm} \delta(t - t_0 - \tau)$  of electron along the arm of the FPI between points of scattering  $x_{1,2}$  (see Appendix). Accumulated phases due to electric and magnetic fields satisfy  $2\pi\phi/\phi_0 = \phi_+ + \phi_-$  and

$$\theta_\pm^{f(b)}(t) = \mp v_D^{-1} \int_{x_1}^{x_2} dx' e\varphi^{f(b)}(t - (x_{2/1} - x')/v_D). \quad (10)$$

We have analyzed the problem in the weak backscattering limit and  $T = 0$  performing the expansion of  $\mathcal{A}_{\text{FPI}}[\varphi]$  up to order of  $|r_j|^2$  in a similar fashion as in Ref. [16]. The intermediate result is quadratic in variables  $\varphi_{r(l)}$  and  $\varphi_i$ , and they can be integrated out. The resulting action then takes a form  $\mathcal{A}_e[\varphi_e] = \mathcal{A}_{RPA} + \mathcal{A}_b$ , where

$$\begin{aligned} \mathcal{A}_{RPA} = & \frac{1}{2} \int_{\mathcal{C}} dt_{1,2} \varphi(t_1) V^{-1}(t_1 - t_2) \varphi(t_2) \\ & - \int_{\mathcal{C}} dt \varphi(t) Q_0(t) - \frac{1}{2} \bar{C}_i^{-1} \int_{\mathcal{C}} dt (Q_i - q_i)^2 \quad (11) \end{aligned}$$

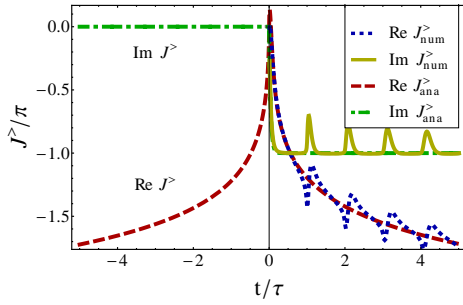


FIG. 4: Correlation function  $J^>$ : comparison of analytic approximation  $J^>_{\text{ana}}$  and numerical results  $J^>_{\text{num}}$  for  $\omega_C \tau = 25$ .

with

$$V^{r/a}(\omega) = \frac{\omega/\bar{C}_e}{\omega \pm i\omega_C(1 - e^{\pm i\omega\tau})} \quad (12)$$

being the effective RPA  $e$ - $e$  interaction and the charge

$$Q_0 = \frac{\nu^* e^2 \tau}{2\pi} (V_+ + V_-) + \bar{C}_e V_g + \frac{\bar{C}_{ei}}{\bar{C}_i} Q_i. \quad (13)$$

The last term of Eq. (11) is just the electrostatic energy (6) of the Coulomb island. The backscattering action (being non-linear in  $\varphi_e$ ) reads

$$i\mathcal{A}_b = \sum_{kl} \int_C dt_{1,2} e^{-2i\Phi(x_k, t_1)} \Pi_{kl}(t_1 - t_2) e^{2i\Phi(x_l, t_2)} \quad (14)$$

with the polarization operators defined as

$$\Pi_{kl}^{\gtrless}(t) = -r_k r_l^* e^{-2i\pi\epsilon_{kl}\phi/\phi_0} f_+^{\gtrless}(\epsilon_{kl}\tau + t) f_-^{\gtrless}(\epsilon_{kl}\tau - t), \quad (15)$$

where  $\epsilon_{kl}$  is the antisymmetric tensor,  $f_\mu^>(t) = \delta(t) - f_\mu^<(t)$ , and the relative phase  $\vec{\Phi} = \hat{D}\sigma_3\vec{\varphi}_e$ . Here we have introduced doublets, e.g.  $\vec{\varphi}_e = (\varphi_e^f, \varphi_e^b)^T$ , and the particle-hole propagator has the conventional structure in Keldysh space with  $\mathcal{D}^{r/a}(\omega; x, x') = \text{sign}(x - x') e^{\pm i\omega|x-x'|/v_D/2v_D}$ .

The backscattering current can be now obtained using the relation  $I_b = e \sum_{ij} (I_{ij}^> - I_{ij}^<)$ , where the forward/backward backscattering rates are represented as the path integral over  $\varphi_e$ ,

$$I_{ij}^{\gtrless} = \int dt \mathcal{D}\varphi_e e^{i\mathcal{A}_e[\varphi_e] - 2i\Phi^{b/f}(x_i, t)} \Pi_{ij}^{\alpha\beta}(t) e^{2i\Phi^{f/b}(x_j, 0)}. \quad (16)$$

The evaluation of this integral requires knowledge of the phase correlator  $D_\Phi \equiv -i\langle \Phi\Phi \rangle = -DVD$ . Using the RPA interaction (12) and the definition of the p-h propagator, given above, one readily obtains

$$D_\Phi^{\gtrless}(t; x_i, x_j) = \frac{iA_{ij}}{8\nu^*} \{J^{\gtrless}(t - \tau) - J^{\gtrless}(t) + (t \rightarrow -t)^*\}, \quad (17)$$

where we have denoted  $A_{ij} = 2\delta_{ij} - 1$  and

$$J^{\gtrless}(t) \equiv \int_0^{\pm\infty} \frac{d\omega}{\omega} \frac{i\omega_C(1 - e^{i\omega\tau})}{\omega + i\omega_C(1 - e^{i\omega\tau})} (e^{-i\omega t} - 1). \quad (18)$$

This integral is accessible only numerically (Fig. 4). However, in the long time limit,  $\omega_C t \gg 1$ , which is consistent with a low bias condition  $eV \ll \omega_C$ , one can use the approximation  $J^{\gtrless}(t) \approx -\ln[-\omega_C(t \mp ia)]$  with a short time cutoff  $a \sim \omega_C^{-1}$ . Logarithmic correlations make this problem essentially similar to the one of tunneling into the non-equilibrium Luttinger liquid with impurity [17]. We have used the real-time instanton method [18] developed in Ref. [17] to evaluate the functional integral (16). It gives the AB phase (5) and the conductance (3) with renormalized reflection coefficients and the bias dependent dephasing rate  $\tau_\varphi^{-1}$  shown in Fig. 2(right).

*Conclusions* — We have presented the theory of electronic Fabry-Perot interferometer (FPI), taking into account  $e$ - $e$  interaction using the simple capacitive network model. We have unraveled the mystery of the diversity in experimental observations of the AB effect in the FPI by presenting the two-parameter “phase diagram” of the device (Table I) discriminating between “Aharonov-Bohm” and “Coulomb-dominated” regimes. The same model predicts the nonequilibrium dephasing rate and the lobe structure for the visibility in agreement with experiment.

We thank I.V. Gornyi, M. Heiblum, A. Mirlin, N. Ofek, D.G. Polyakov, S. Carr, and A. Stern for useful discussions. This work was supported by EUROHORCS/ESF, by GIF Grant No. 965 and by CFN/DFG.

- 
- [1] D. T. McClure *et al.*, Phys. Rev. Lett. **103**, 206806 (2009).
  - [2] Yiming Zhang *et al.*, Phys. Rev. B **79**, 241304(R) (2009).
  - [3] Y. Yamauchi *et al.*, Phys. Rev. B **79**, 161306(R) (2009).
  - [4] N. Ofek *et al.*, Proc. Natl. Acad. Sci. USA **107**, 5276 (2010).
  - [5] Y. Ji *et al.*, Nature (London) **422**, 415 (2003).
  - [6] C. Nayak *et al.*, Rev. Mod. Phys. **80**, 1083 (2008).
  - [7] C. de C. Chamon *et al.*, Phys. Rev. B **55**, 2331 (1997).
  - [8] B. Rosenow and B. I. Halperin, Phys. Rev. Lett. **98** 106801 (2007).
  - [9] B. I. Halperin *et al.*, Phys. Rev. B **83**, 155440 (2011).
  - [10] D.B. Chklovskii, K.A. Matveev, and B.I. Shklovskii, Phys. Rev. B, **47**, 12605 (1993).
  - [11] N.R. Cooper and J.T. Chalker, Phys. Rev. B **48**, 4530 (1993).
  - [12] A. Furusaki and K.A. Matveev, Phys. Rev. B **52**, 16676 (1995); D. A. Bagrets and Yu. V. Nazarov, Phys. Rev. Lett. **94** 056801 (2005).
  - [13] A. Grishin, I.V. Yurkevich, I.V. Lerner, Phys. Rev. B **69**, 165108 (2004) and references therein.
  - [14] I. Snyman and Yu. V. Nazarov, Phys. Rev. B **77**, 165118 (2008).
  - [15] L. S. Levitov, H.-W. Lee, and G. B. Lesovik, J. Math. Phys. **37**, 4845 (1996).
  - [16] M. Schneider, D. A. Bagrets, and A. D. Mirlin, arXiv:1101.4391.
  - [17] S. Ngo Dinh, D. A. Bagrets, and A. D. Mirlin, Phys. Rev. B **81**, 081306(R) (2010).
  - [18] See supporting online material.

## SUPPORTING ONLINE MATERIAL

### Scattering matrix of the FPI

In order to construct the scattering matrix in Eq. (9) we need to identify the two main constituents of single-particle dynamics:

- (a) scattering at QPC  $j$ ,  $s_j = \begin{pmatrix} t_{j++} & r_{j+-} \\ r_{j-+} & t_{j--} \end{pmatrix}$ ,  $j = 1, 2$ ;
- (b) propagation in between, along the lower/upper edge,  $\mathcal{M}_\pm(t, t_0) = e^{i\theta_\pm(t) + i\phi_\pm} \delta(t - t_0 - \tau)$ .

Summing up all possible trajectories then gives the total scattering matrix  $S[\varphi^\alpha] = \begin{pmatrix} T_{++} & R_{+-} \\ R_{-+} & T_{--} \end{pmatrix}$ . Electrons can encircle the interferometer an arbitrary number of times, each turn giving rise to an amplitude of  $r_{1+-}\mathcal{M}_-r_{2-+}\mathcal{M}_+$ . The corresponding geometric series gives  $R_\infty = [1 - r_{1+-}\mathcal{M}_-r_{2-+}\mathcal{M}_+]^{-1}$  such that e. g.

$$\begin{aligned} R_{-+} &= r_{1-+} + t_{1--}\mathcal{M}_-r_{2-+}\mathcal{M}_+R_\infty t_{1++}, \\ T_{++} &= t_{2++}\mathcal{M}_+R_\infty t_{1++}, \end{aligned}$$

where the dependence of  $\mathcal{M}_\pm$  and hence of  $S$  on the configuration  $\varphi$  has been left implicit.

### Saddle point approximation

We use the real-time instanton method developed in Ref. [17] to evaluate the functional integral (16). Optimizing the tunneling action

$$\mathcal{A}_{ij} = \mathcal{A}_e[\varphi_e] - 2i\Phi^\alpha(x_i, t_1, [\varphi_e]) + 2i\Phi^\beta(x_j, t_2, [\varphi_e]) \quad (19)$$

with respect to  $\varphi_e$  one obtains the approximate saddle-point  $\varphi_e^*$ , and the related phase

$$\begin{aligned} \Phi_*^\gamma(t, x) &= \langle \Phi^\gamma(t, x) [-2i\Phi^\alpha(t_1, x_i) + 2i\Phi^\beta(t_2, x_j)] \rangle \\ &\quad + \Phi_0(x) \quad (20) \end{aligned}$$

where the dependence on  $\alpha$ ,  $\beta$ ,  $x_i$ ,  $x_j$ ,  $t_1$ , and  $t_2$  has been left implicit. The phases  $\Phi_0(x_{1,2})$  are accumulated by electrons in the mean electrostatic potential on the interfering channels,

$$\Phi_0(x_{1,2}) = \mp \frac{\pi Q_0}{\nu^* e} \left( \frac{\omega_C \tau}{1 + \omega_C \tau} \right), \quad (21)$$

where the charge  $Q_0$  was defined in Eq. (13).

A substitution of the stationary phase (20) into the tunneling action  $\mathcal{A}_{ij}$  renormalizes the backscattering polarization operators in Eq. (16),

$$\tilde{\Pi}_{kl}^{\gamma\delta}(t) = \Pi_{kl}^{\gamma\delta}(t) \exp \left\{ -2 \left\langle (\Phi_k^\gamma(t) - \Phi_l^\delta(0))^2 \right\rangle \right\}, \quad (22)$$

thereby changing their singular behaviour to

$$\tilde{\Pi}_{kl}(t) \sim e^{-ieVt} t^{-2-2\lambda} (t^2 - \tau^2)^\lambda. \quad (23)$$

The exponents here are  $\lambda = -1/2\nu^*$  for  $k = l$  and  $\lambda = 1/2\nu^* - 1$  for  $k \neq l$  (thus, they assume their non-interacting values in the limit  $\nu^* \rightarrow \infty$ ). To obtain the same renormalization in the backscattering action (14) one should take into account the quantum fluctuations around the saddle-point trajectory  $\Phi_*^\gamma$ .

We concentrate on the limit of large bias,  $\omega_C \tau \gg |eV\tau| \gg 1$ , where the singularities of the ‘‘dressed’’ polarization operator  $\tilde{\Pi}(t)$  dominate the real-time integrals in Eqs. (14), (16) and restrict ourselves to the case  $\nu^* > 1$ . For each of the interference current contribution,  $I_{12}$  and  $I_{21}$ , the most essential part of the integral come from two singularities at  $t \simeq \pm\tau$ . Summing up these four terms one obtains the result (2) with the AB phase

$$\varphi_{AB} = 2\pi\phi/\phi_0 + e(V_+ + V_-)\tau + \Phi_0(x_1) - \Phi_0(x_2). \quad (24)$$

Using the relation (21) one can verify that in the limit  $\omega_C \tau \gg 1$  which we consider the phase  $\varphi_{AB}$  indeed coincides with the one given by Eq. (5).

On the other hand, the backscattering action evaluated on the saddle-point  $\Phi_*^\gamma(t, x)$  is dominated by the incoherent terms  $k = l$  around  $t_1 \simeq t_2$  in Eq. (14). They give rise to out-of-equilibrium dephasing due to quantum shot noise,  $i\mathcal{A}_b[\varphi_e^*] = -\tau/\tau_\varphi$ , with the voltage dependent rate  $\tau_\varphi^{-1}$  shown in Fig. 2(right).

Incoherent corrections to the current,  $I_{ii}$ , are dominated by the singularities of Eq. (16) at  $t \rightarrow 0$ , yielding the total classical conductance

$$g_{cl} = \nu - (R_{1*}(V) + R_{2*}(V)). \quad (25)$$

The applicability of the weak backscattering limit requires the renormalized reflection coefficient to satisfy  $R_{j*}(\epsilon_{Th}) \ll 1$ , which means that the Coulomb blockade on the FPI has not yet developed. This gives a condition  $|r_j| \ll 1/(\omega_C \tau)^{1/2\nu^*}$  on initial values of the backscattering amplitudes in our model.